SI cooling – 16/04/2026

The Spin Thermoelectric Effect in Nonmagnetic Chiral Materials

Sheli Muzafe Reiss,[1] Clement Gedeon, [2,3,4] Ohad Golan,[1] Ofek Vardi [1,9] ,Dror Merhav, [1] Christos L. Chochos,[2,5] Shira Yochelis,[1] David H. Waldeck,[6] Jonas Fransson, Jeanne Crassous[3,], Ron Naaman,[7*] and Yossi Paltiel.[1*]*

[1] *Applied Physics Department and Center for Nano-Science and Nano-Technology, The Hebrew University of Jerusalem, Jerusalem 9190401, Israel.*

[2] Advent Technologies SA, Stadiou Str, Platani 26504, Patras, Greece.

[3] Univ Rennes, CNRS, ISCR – UMR 6226, 35000 Rennes, France.

[4] Current address: LCPO Bordeaux, CNRS - UMR 5629, 33615 Pessac, France.

[5] Current address: Institute of Chemical Biology National Hellenic Research Foundation, Athens 11635, Greece.

[6] Department of Chemistry, University of Pittsburgh, Pittsburgh, Pennsylvania 15260, United States.

[7] Department of Physics and Astronomy, Box 516, 751 21, Uppsala University, Uppsala, Sweden.

[8] Department of Chemical and Biological Physics, Weizmann Institute, Rehovot 7610001, Israel.

[9] *The Racah Institute of Physics, The Hebrew University of Jerusalem, Jerusalem 91904, Israel*

Ion implantation profile

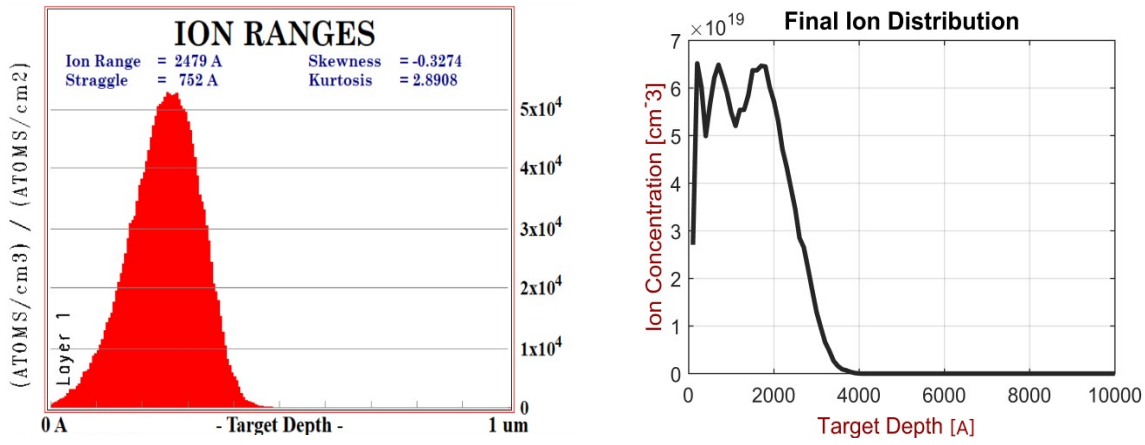

Figure S1. *(a) Example of SRIM simulation of ion distribution at 150 keV. (b) Final optimized profile simulation, obtained via multi-energy implantation.*

Lithograph steps

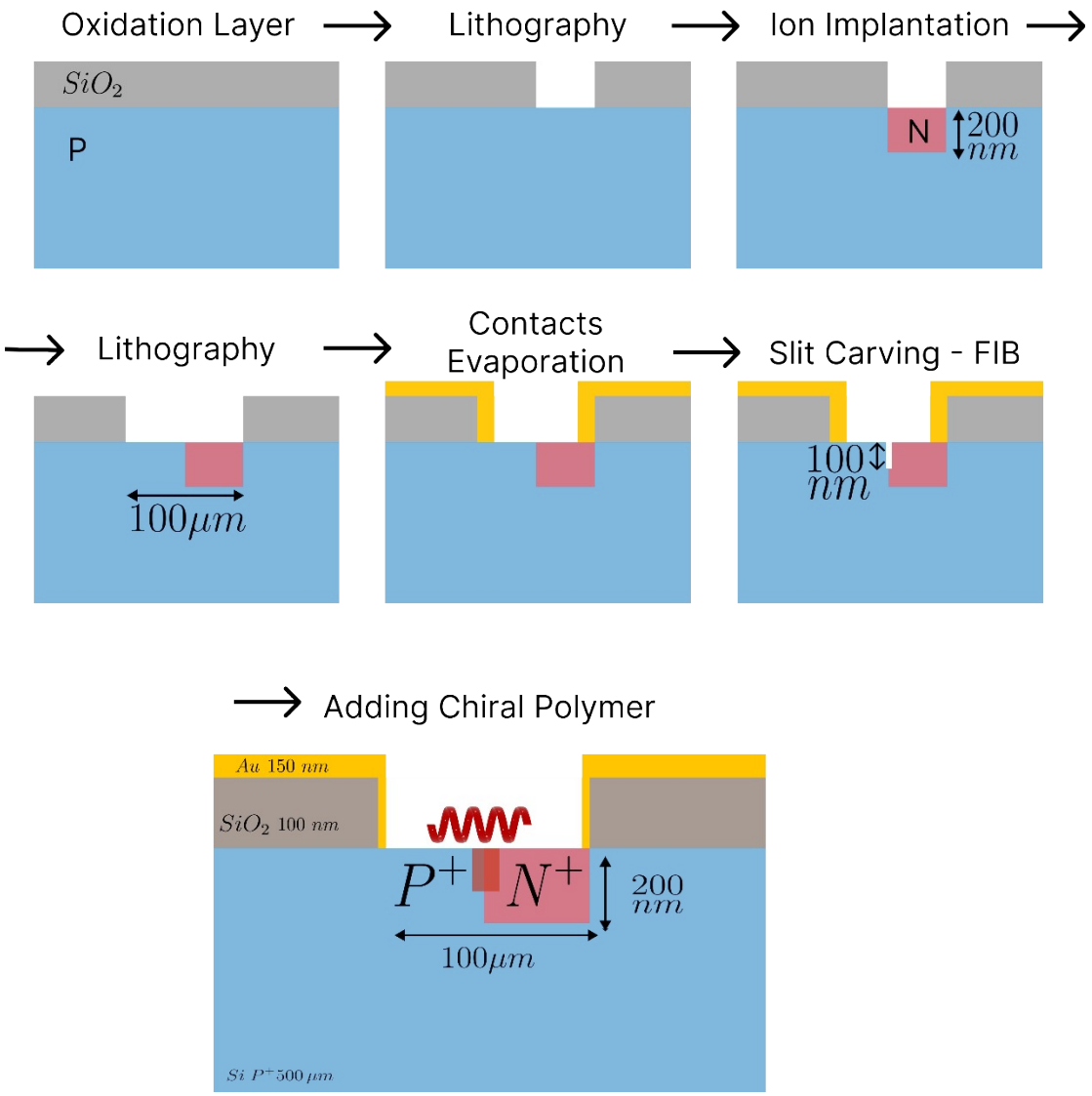

Figure S2. *Illustration of the device fabrication process at different process steps, with the final device parameters in the final step.*

Polymer profile

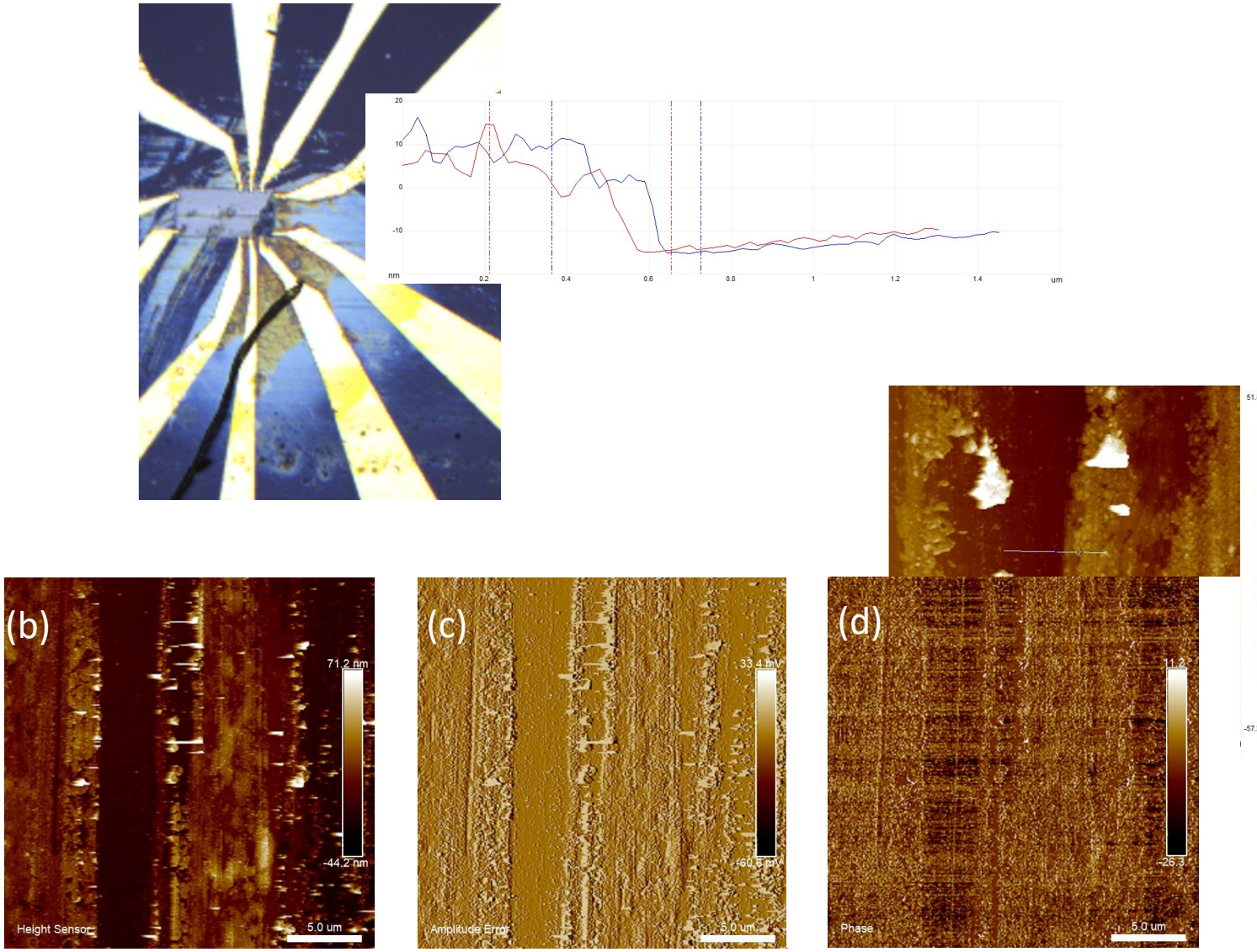

Figure S3 (a) *Image of the device with electrodes connected to the P-N junctions that are filled with the polymer. For the polymer height analysis above the slit half of the device was cleaned. The cleaned area is denoted as dark blue and the area with the polymer is denoted as bright blue. Using tapping AFM to measure the polymer's height, the thickness of the polymer above the slit was found to be around 20nm averaging 6 similar cuts (see the two profiles above). Therefore, the total thickness of the polymer is around 220nm. (b-d) AFM measurements of the chiral polymer on the p-n junction device are shown, focusing on a region where a slit was intentionally scratched to expose the underlying substrate. (b) The topography image reveals a striped morphology, where the scratched region appears as elongated depressions relative to the surrounding polymer-covered areas. This contrast enables identification of the slit and distinguishes it from the intact polymer film. (c) The amplitude error image emphasizes these features, highlighting sharp transitions at the boundaries of the slit and confirming the presence of abrupt changes in the surface profile along the scratched region. (d) The phase image exhibits contrast that follows the striped morphology, with a consistent difference between the slit and the surrounding film. This contrast indicates a change in tip–sample interaction between the exposed substrate and*

the polymer-covered areas, supporting the identification of the two regions and suggesting differences in their local mechanical or adhesive properties.

IV curves

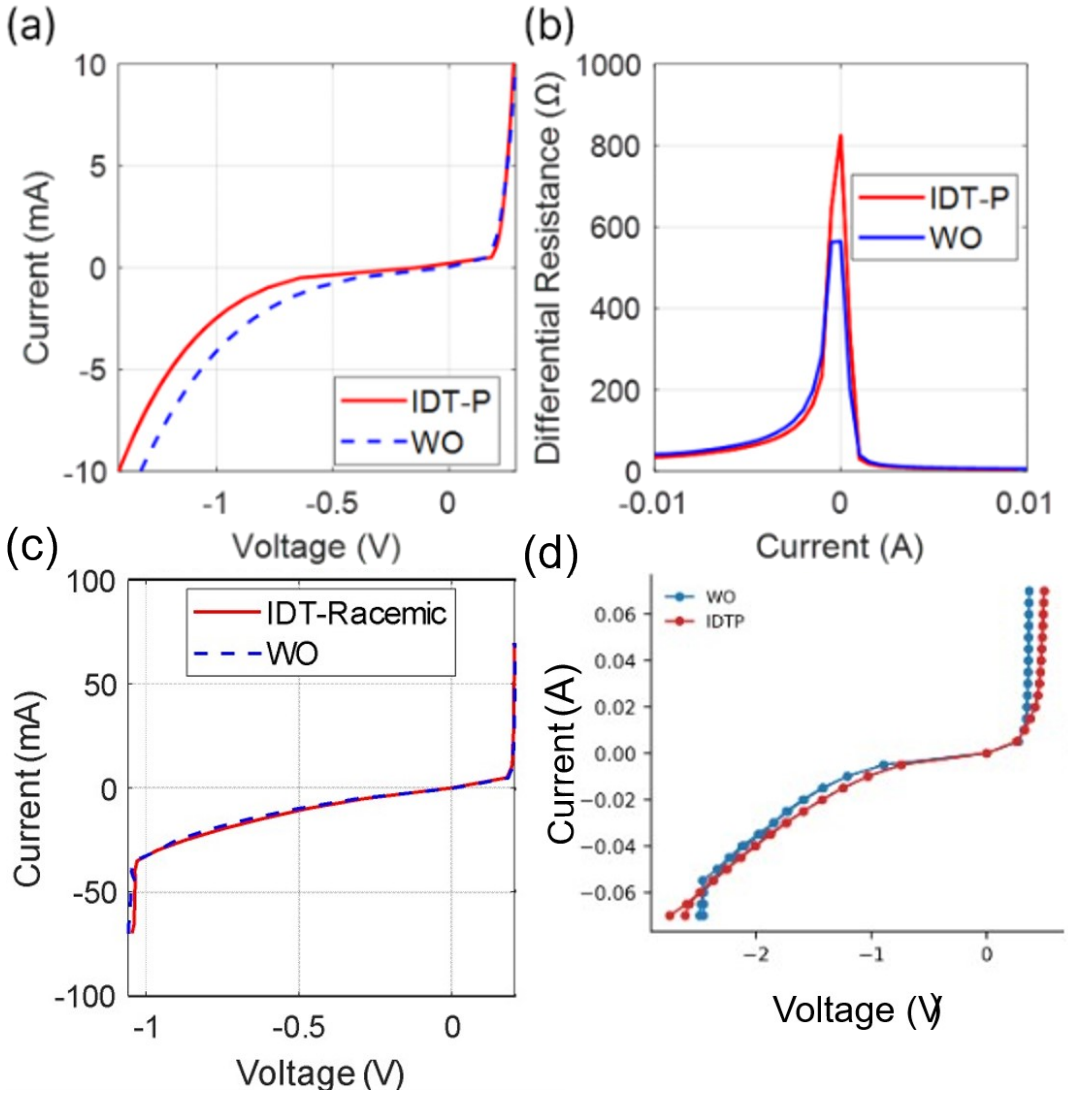

Figure S4. *(a) IV curve for a different bare device with and without IDT-P. (b) Differential resistance for the bare device and with IDT-P, showing no significant change for high currents. (c) Extended range IV curve for a different bare device with and without IDT-Racemic. (d) Extended range IV curve for a different bare device with and without IDT-P.*

Comparison of Enantiomers

(a)

(b)

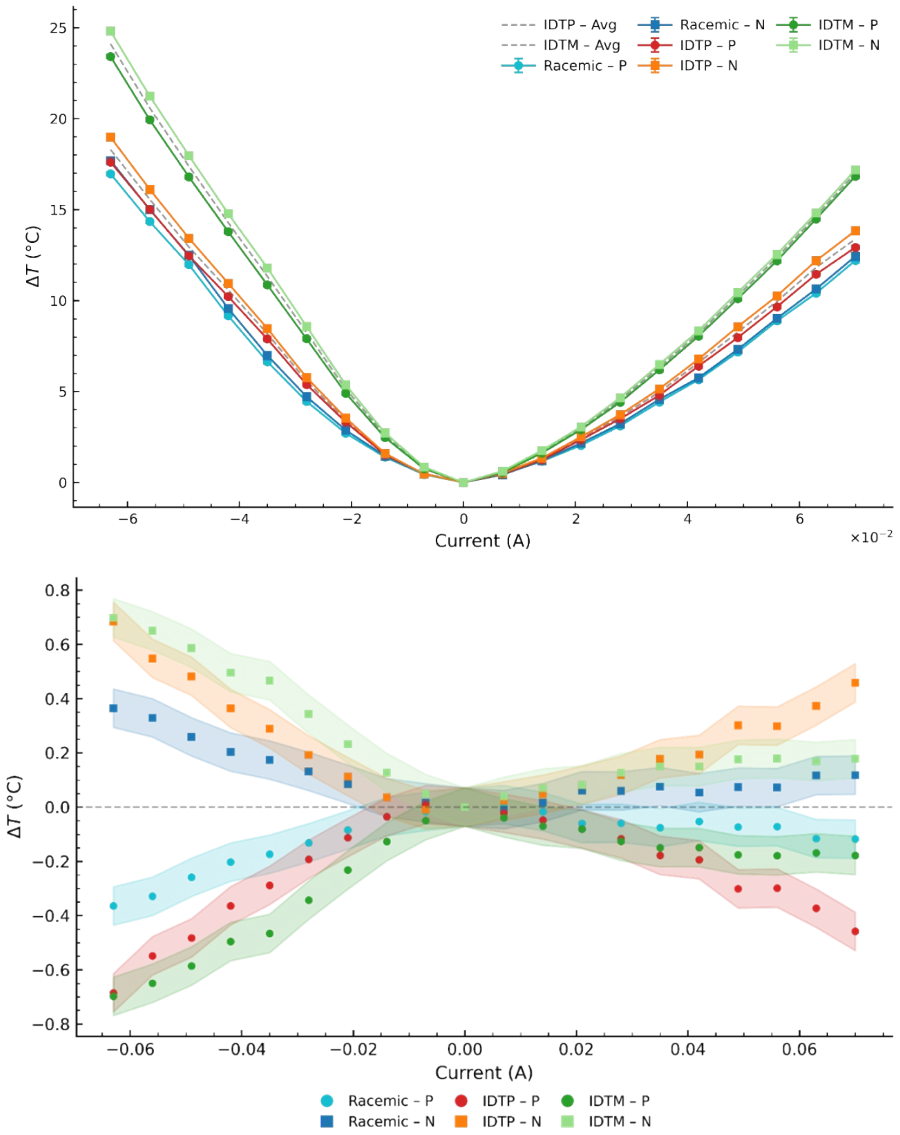

Figure S5. (a) *Comparison of the temperature change on the n and p sides as a function of input current, for a p-n junction device with the chiral polymer IDT-Hel-P-50 (IDTP), IDT-Hel-M-50 (IDTM), and a racemic polymer mixture (Racemic).(b) Temperature difference between the P and N contacts normalized by the average device temperature for the IDTP, IDTM, and racemic versions. Both enantiomers exhibit a double temperature gradient, compared to the racemic version.*

A highly conservative approach was used to estimate the temperature uncertainty. We calculated the total error bars as the geometric sum of the systematic instrument limit and the random temporal noise:

1. *Instrument Error: We included a baseline uncertainty of 0.1 °C. This is based on the Noise Equivalent Temperature Difference (NETD) specifications of our thermal camera (Optris Xi 400), serving as a conservative upper bound for the detection limit.*

2. *Standard Error: To this, we added the standard error of the mean calculated over a 15-second steady-state measurement period (comprising approximately 150 individual frames).*

Heat Flow Measurement

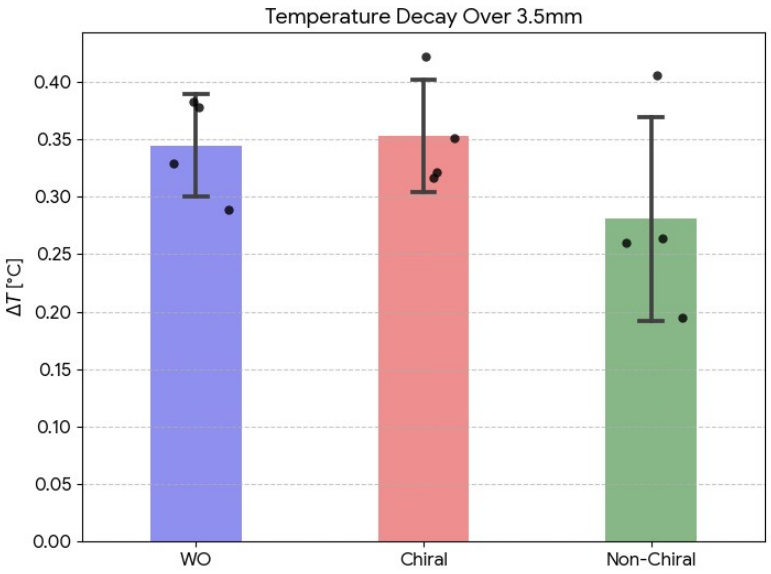

Figure S6. *Temperature decay over 3.5mm on a Tantalum substrate with heating applied on one side. Without added molecules (blue), chiral α-helix (orange), and non-chiral MUP alkyl thiol (green) surfaces. The surfaces were temperature recorded over time using a thermal camera. MUP alkyl thiol has been used as a non-chiral analog to the used α-helix.*

A difference in temperature decay could be seen between the chiral and non-chiral surfaces. This indicates a difference in heat flow, which might contribute to the effects described in the paper.

Better understanding this concept is a subject for future work.